Astron. Astrophys. 345, 391–402 (1999)

ASTRONOMY AND ASTROPHYSICS

The emission line sequence of normal spiral galaxies

L. Sodré Jr.[1] **and G. Stasińska**[2]

[1] Departamento de Astronomia, Instituto Astronômico e Geofísico da USP, Av. Miguel Stefano 4200, 04301-904 São Paulo, Brazil (laerte@iagusp.usp.br)
[2] DAEC, Observatoire de Meudon, F-92195 Meudon Principal Cedex, France (grazyna@obspm.fr)

Received 5 October 1998 / Accepted 2 March 1999

Abstract. We have analyzed the emission line properties in the integrated spectra of 15 normal spiral galaxies. We show that very clear trends appear when plotting relevant emission line ratios or equivalent widths as a function of galaxy spectral types, obtained with a Principal Component Analysis of the continua and absorption features of spectra. The equivalent widths of all the lines analyzed correlate extremely well with spectral types, implying that each of them can be considered a good indicator of the spectral type in normal galaxies. The position of most galaxies of our sample in classical emission line diagnostic diagrams follows that of individual giant HII regions in spiral galaxies, but for the earliest type galaxies, the emission line pattern resembles more that of LINERs. Therefore, the direct interpretation of equivalent widths in terms of star formation rates would be misleading in such cases. The observed trends in the emission line ratios as a function of galaxy spectral type suggest a decrease of O/H, a decrease of N/O, an increase of the average effective temperature or ionization parameter, and a decrease of the effective internal extinction of galaxies with increasing (early to late) spectral type.

Key words: methods: statistical – galaxies: fundamental parameters – galaxies: ISM – galaxies: active – galaxies: spiral

1. Introduction

Emission lines in normal galaxies are powerful tracers of the physical processes associated with the galaxy interstellar medium and the formation of massive stars. They allow quantitative estimates of the star formation rates, as well as of the chemical abundances and physical conditions of the gas in galaxies (McCall et al. 1985; Gallagher et al. 1989; Kennicutt et al. 1994; Zaritsky et al. 1994; Barbaro & Poggianti 1997).

A census of emission line properties in integrated spectra of normal galaxies is particularly interesting in view of studies of galaxies at large redshifts, too distant to be spatially resolved. It provides useful information also for nearby galaxies, as it allows investigating the global properties of their emission. It is well known that emission lines tend to become more prominent as one goes from early to late galaxy types, and the degree to which the spiral arms are resolved into individual HII regions (where most of the emission lines in normal galaxies are produced) is one of the most important criteria for discriminating among the spiral types in the Hubble system (Hubble 1936; Sandage 1961). Kennicutt (1992a, hereafter K92a) has already discussed some properties of the emission lines in integrated spectra, mainly evaluating their reliability as quantitative tracers of the total massive star formation rate in galaxies. Lehnert & Heckman (1994) have examined the location of integrated spectra of galaxies in the standard emission line diagnostic diagrams used to classify emission line objects (Baldwin et al. 1981; Veilleux & Osterbrock 1987), concluding that the integrated emission in star-forming galaxies has a substantial contribution of a diffuse component, with physical properties different from those found in high surface brightness HII regions. Most studies, however, have focused on the properties of emission lines produced either in HII regions in the spiral arms of disk galaxies (e.g. McCall et al. 1985; Belley & Roy 1992; Oey & Kennicutt 1993; Zaritsky et al. 1994; Kennicutt & Garnett 1996; Roy & Walsh 1997) or in galactic nuclei (Heckman et al. 1980; Keel 1983; Ho et al. 1997). In particular, Zaritsky et al. (1994) have investigated the oxygen abundance properties of a sample of disk galaxies from the spectra of individual HII regions located at various galactocentric radii. They found that the characteristic abundance of the galaxies correlates well with both their morphological type and their luminosity.

In this paper we examine the trends of emission line properties in the *integrated* spectra of 15 normal, nearby spiral galaxies. The spectra come from Kennicutt's (1992b, hereafter K92b) spectro-photometric atlas.

The galaxies are ordered by galaxy spectral type (hereafter ST), obtained using Principal Component Analysis of the integrated properties of the continua and absorption features of 23 normal galaxies of all morphologies, in a manner similar to the one introduced by Sodré & Cuevas (1994, 1997) and several other authors (e.g., Connolly et al. 1995; Zaritsky et al. 1995; Folkes et al. 1996; Galaz & de Lapparent 1998). Such a procedure allows to define a spectral classification that correlates well with Hubble morphological types and present some advantages over the usual morphological classification. Firstly, it provides quantitative, continuous, and well defined types, avoiding the

Send offprint requests to: L. Sodré Jr.

ambiguities of the intrinsically more qualitative and subjective morphological classification. Secondly, the sequence of galaxies obtained in this way is easier to model than the Hubble sequence, because the physical process behind galaxy spectra are better understood than those needed to explain galaxy morphologies. Thirdly, this classification can be applied to redshift surveys where no information is available on the galaxy morphologies, allowing to "recycle" data obtained for other purposes (de Lapparent et al. 1998; Bromley et al. 1998).

We will show that the patterns of variation of emission line properties along the sequence of normal galaxies are much more regular when considering the galaxy spectral type sequence than when using the morphological sequence.

This paper is organized as follows. In Sect. 2 we introduce the sample of normal galaxies, briefly describe the procedure used to obtain spectral types from integrated galaxy spectra, and present the relevant data for the emission lines in the blue/visible region of the spectra. In Sect. 3 we present the trends of equivalent widths and emission line ratios with galaxy spectral types. In Sect. 4 we interpret these trends, after a brief reminder on emission line theory and a comparison of the loci of integrated galaxy spectra with those of giant HII regions in classical diagnostic diagrams. Finally, in Sect. 5 we summarize our results.

Table 1. Standard galaxies and classification

Name	Hubble type	T-type	spectral type	nuclear types
NGC 3379	E0	-5	-5.2	
NGC 4472	E1/S0	-4	-5.7	
NGC 4648	E3	-5	-4.4	
NGC 4889	E4	-5	-4.1	
NGC 3245	S0	-2	-4.6	
NGC 3941	SB0/a	0	-2.7	
NGC 4262	SB0	-2	-3.8	
NGC 5866	S0	-2	-4.4	
NGC 1357	Sa	1	-2.0	
NGC 2775	Sa	1	-3.4	
NGC 3368	Sab	2	-3.3	L2
NGC 3623	Sa	1	-4.1	L2:
NGC 1832	SBb	3	2.4	
NGC 3147	Sb	3	0.0	S2
NGC 3627	Sb	3	1.4	T2/S2
NGC 4775	Sc	5	9.7	
NGC 5248	Sbc	4	1.4	H
NGC 6217	SBbc	4	4.8	H
NGC 2903	Sc	5	1.1	H
NGC 4631	Sc	5	9.4	H
NGC 6181	Sc	5	3.1	H
NGC 6643	Sc	5	3.8	H
NGC 4449	Sm/Im	9	10.8	H

2. The data base

2.1. The sample of galaxies

The integrated spectra of galaxies discussed in this work come from the atlas of Kennicutt (K92b). They are suitable for setting the basis of a global characterization of galaxies because this is the largest sample of integrated spectra of low-redshift galaxies available and obtained in a uniform way. From this atlas we, conservatively, rejected all the galaxies showing any evidence of strong spectral peculiarities or interactions (i.e. AGNs, starbursts and mergers). This left us with a total of 23 normal galaxies, which will be our standards. They are presented in Table 1, together with their Hubble types (taken from K92a), their T-types (following the RC3 convention- de Vaucouleurs et al. 1991), their spectral types (see below), and the spectral classification of their nuclei according to Ho et al. (1997; see Sect. 4). These galaxies are all at high Galactic latitude, so foreground absorption by our Galaxy is unimportant. Note that the set of standards adopted here is very similar to those used to characterize normal galaxies in other studies of spectral classification (e.g. Folkes et al. 1996; Galaz & de Lapparent 1998).

2.2. The spectral classification

Our general approach to spectral classification is described in detail in Sodré & Cuevas (1997) and in Cuevas et al. (1998). Here we only present an overview of the procedures used to obtain spectral types for the galaxies discussed here. The point to be stressed is that the spectra of normal galaxies form a sequence- the spectral sequence- in the spectral space spanned by the M-dimensional vectors that contain the spectra, each vector being the flux of a galaxy (or a scaled version of it) sampled at M wavelengths (Sodré & Cuevas 1994, 1997; Connolly et al. 1995; Folkes et al. 1996). The spectral sequence correlates well with the Hubble morphological sequence, and we define the spectral type of a galaxy from its position along the spectral sequence.

The spectral sequence is identified using Principal Component Analysis (PCA). PCA allows to define a new orthonormal reference system in spectral space, centered at the baricenter of galaxy spectra and with basis-vectors (the principal components) spanning directions of maximum variance. The plane defined by the first two principal components- which we call principal plane- is the plane that contains the maximum variance in the spectral space.

PCA was applied to a pre-processed version of the 23 original galaxy spectra. Firstly, the spectra were shifted to the rest frame and re-sampled in the wavelength interval from 3784 Å to 6500 Å, in equal-width bins of 2 Å. Secondly, we removed from the analysis 4 regions of $\sim$20 Å each centered at the wavelengths of He II λ4686, Hβ λ4861, [O III] λ4959 and [O III] λ5007. This was done in order to avoid the inclusion of emission lines in the analysis, that increases the dispersion of the spectra in the principal plane (mainly due to an increase in the second principal component). The spectra, now sampled at $M = 1277$ wavelength intervals, were then normalized to the same mean flux ($\sum_\lambda f_\lambda = 1$). After, we computed a mean spectrum and, finally, we subtracted this mean spectrum from the spectrum of each galaxy. PCA was then used to obtain the principal components. This procedure is equivalent to the conventional PCA on the covariance matrix, that is, the basis vectors are the eigenvectors of a covariance matrix. Note that the principal components

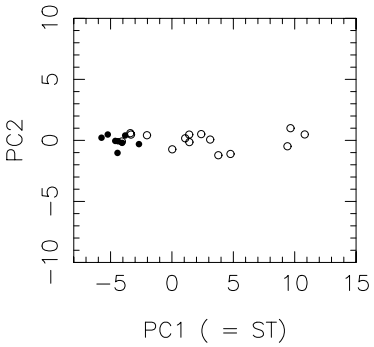

Fig. 1. Projection of the spectra of the 23 standard galaxies on to the principal plane. The spectral sequence follows the first principal component, and a spectral type is attributed to each galaxy by its value of this component. Filled symbols: E and S0 galaxies; open symbols: S galaxies.

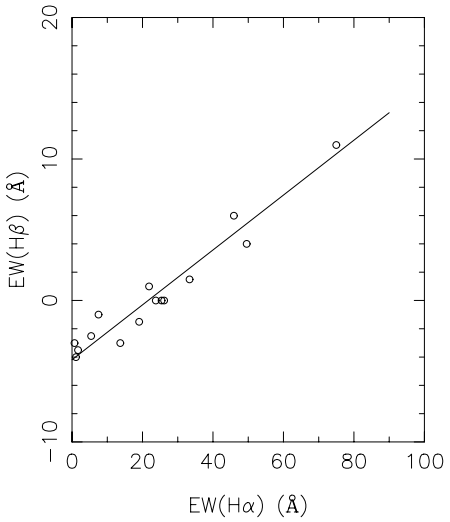

Fig. 2. Relation between the observed values of the equivalent widths of Hα and Hβ. The straight line corresponds to the fitting given by Eq. 1.

are dependent on the data and its pre-processing, and using a different normalization for the spectra or taking some other wavelength interval certainly would lead to a different result for the values of the principal components. However, it can be shown that, to a large extent, these solutions are equivalent, all producing essentially the same ranking of galaxies along the first principal component.

Fig. 1 shows the projection of the spectra of the 23 standards on to the principal plane. This plane is highly informative about the structure of the spectral space, as it contains 94.8% of the data variance. The spectral sequence is readily identified along the first principal component. We then define quantitatively the spectral type ST of a galaxy by the value of its first principal component. These values are presented in Table 1. Note that ST increases from early to late types. In what follows, the spectral sequence will refer to that obtained with the 23 standards of Table 1. The mean values and dispersions of ST for the standards are -4.9 $\pm$ 0.8 for E-E/S0, -3.9 $\pm$ 0.9 for S0-S0/a, -3.2 $\pm$ 0.9 for Sa-Sab, 2.0 $\pm$ 1.8 for Sb-Sbc, and 6.3 $\pm$ 4.1 for Sc-Im. The ranking of spectral types in these groups is analogous to the ranking of Hubble morphological types. Note that the dispersion of ST around the mean value of each group is large enough to produce a substantial overlap in the spectral sequence of galaxies of different Hubble types: galaxies of same morphologies may have very different spectral types.

It is worth emphasizing that we base our spectral classification only on the integrated properties of the stellar populations that are contained in the continuum and absorption lines, and that the emission lines enter in no way in the classification scheme.

2.3. Emission line data and reddening correction

Among our 23 standard galaxies, emission lines are measured only for the 15 spirals ($T \geq 1$), being too weak or undetected in the integrated spectra of galaxies of earlier types (at the resolution of the observations, $\sim$5–7 Å; see K92b). We use all the emission lines with equivalent widths (EW) measured by K92a: [OII]λ3727, Hβ, [OIII]λ5007, Hα, [NII]$\lambda\lambda$6548, 6583, and [SII]$\lambda\lambda$6717, 6731. The EW of Hα was computed from the EW of Hα+[NII] and the value of [NII]/Hα, also from K92a. Other emission lines, like [OI]$\lambda\lambda$6300,6363, are not strong enough to be reliably measured in the spectra of Kennicutt's atlas (K92b).

In the next sections we will discuss the behavior of reddening corrected line ratios. For that, we have obtained a value of the effective internal reddening of the galaxies from an estimation of the emission line intensity ratio of Hα and Hβ, Hα/Hβ. Our procedure is similar to the one adopted by K92a. We begin by modeling the relation between the observed EWs of Hα and Hβ by a straight line (Fig. 2). Using the bisector estimation for the fitting (Isobe et al. 1990), we have obtained

$$\mathrm{EW(H}\beta)_{obs} = -4.19(\pm0.36) + 0.194(\pm0.011)\mathrm{EW(H}\alpha)_{obs} \quad (1)$$

Note that this linear relationship is purely empirical, and there is not, *a priori*, any reason for EW(H$\beta)_{obs}$ and EW(H$\alpha)_{obs}$ be linearly related.

The observed EW of a line may be written as EW$_{obs}$=EW$_{em}$+EW$_{abs}$, where EW$_{em}$ is the emission component (> 0) and EW$_{abs}$ corresponds to the component due to stellar absorption (< 0). To proceed, we need to know how EW$_{abs}$ behaves as a function of EW$_{em}$ or EW$_{obs}$. Let us suppose, then, that the emission and observed EWs of Hα and Hβ may also be related linearly, which is a reasonable assumption in most models (e.g., Barbaro & Poggianti 1997). Writing EW(H$\alpha)_{em} = a_\alpha + b_\alpha$EW(H$\alpha)_{obs}$ and EW(H$\beta)_{em} = a_\beta + b_\beta$EW(H$\beta)_{obs}$, and substituting these relations in Eq. 1, we obtain EW(H$\beta)_{em} = C + R$ EW(H$\alpha)_{em}$, where C and R are constants. Now, physical solutions require C equal to zero, because EW(H$\beta)_{em}$ should go to zero when EW(H$\alpha)_{em}$ goes to zero. Consequently, we obtain that the emission EWs of Hα and Hβ are related by

$$\mathrm{EW(H}\beta)_{em} = R\,\mathrm{EW(H}\alpha)_{em} \quad (2)$$

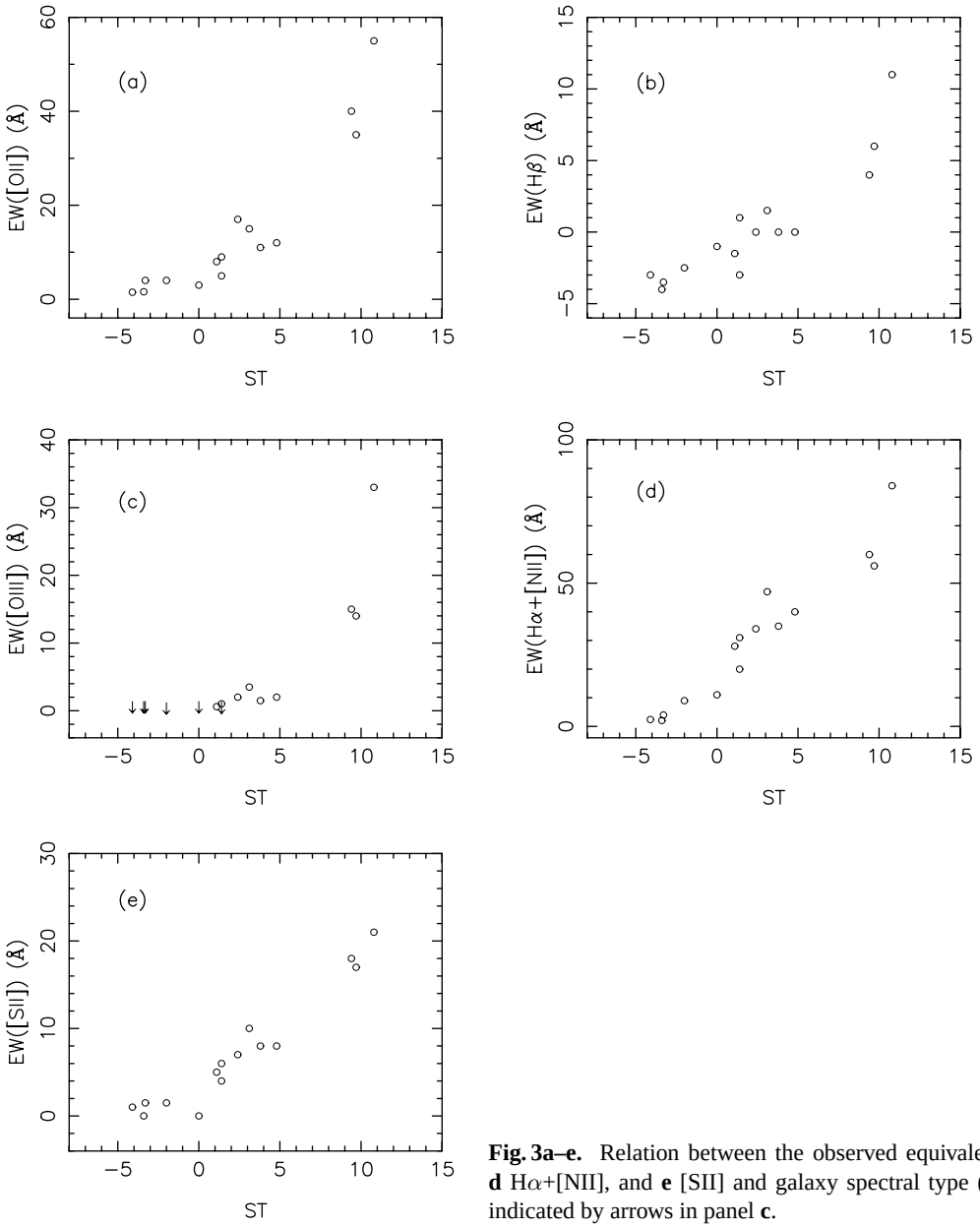

Fig. 3a–e. Relation between the observed equivalent widths of **a** [OII], **b** Hβ, **c** [OIII], **d** Hα+[NII], and **e** [SII] and galaxy spectral type (ST). Upper values of EW([OIII]) are indicated by arrows in panel **c**.

with $R = 0.194 b_\beta / b_\alpha$. With these assumptions, Hα/Hβ depends only on R and the ratio of the continuum fluxes at Hα and Hβ, that we have measured in the spectra. We have adopted here $R = 0.2$, since models like those of Barbaro & Poggianti (1997) indicate that $b_\beta \sim b_\alpha$.

The extinction coefficient at Hβ, $C(\mathrm{H}\beta)$, has been computed assuming an intrinsic value for Hα/Hβ of 2.9 (corresponding to an electron temperature of 9000 K in the case B of the theory of recombination-line radiation). The expected formal error in $C(\mathrm{H}\beta)$ from this procedure is ~ 0.18. The values of $C(\mathrm{H}\beta)$ may be considered a crude estimation of the global extinction in the galaxies, since, as mentioned above, foreground extinction by our Galaxy is negligible.

It is important to stress that, although very simple, this estimate of the reddening is quite robust, and there is not any evidence in the data that a more complex model is required. As we shall see, it leads to a Hα/Hβ ratio that decreases steadily with spectral type. We have verified that this trend continues when other ways to estimate the reddening are used. Also, the behavior of other line ratios discussed in the next sections are, to a large extent, not strongly affected by the use of other values of R.

3. Trends of emission line properties with galaxy spectral type

3.1. Equivalent widths

Fig. 3 consists of 5 panels showing the behavior of the observed EWs of [OII], Hβ, [OIII], Hα+[NII] and [SII] as a function of ST. In all of them we see a clear increase of the emission line

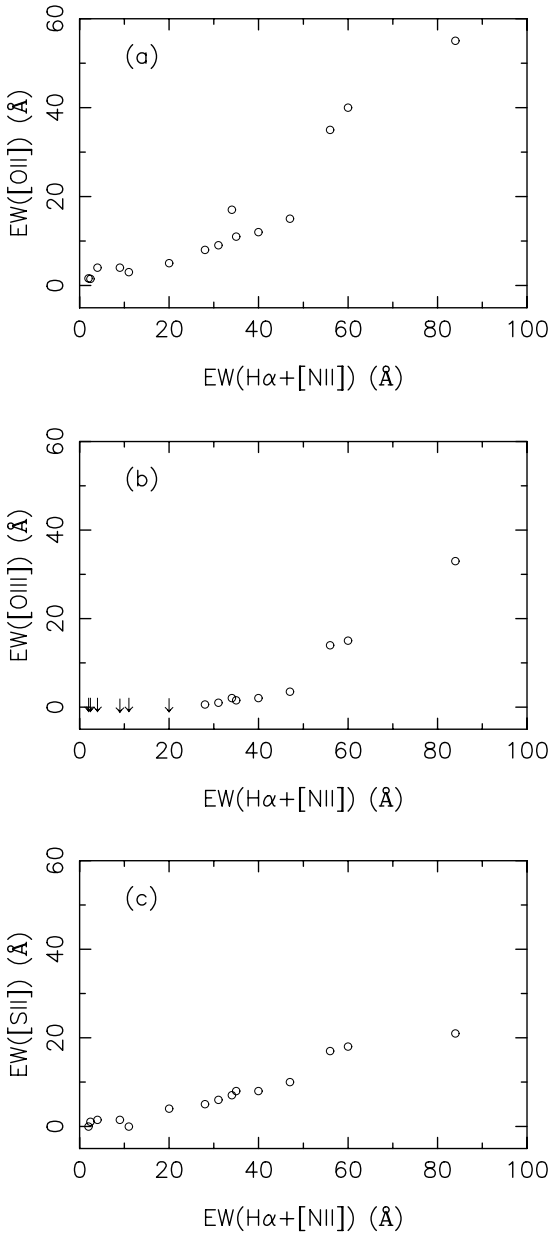

Fig. 4a–c. Relation of the observed equivalent widths of **a** [OII], **b** [OIII], and **c** [SII] with EW(Hα+[NII]).

EWs as a function of the galaxy spectral type. For [OIII], the increase is apparent only from ST=2 upwards, since this line is too weak to be effectively measured in spectral types lower (i.e., earlier) than that. We had shown, in Fig. 2, the relation between EW(Hβ) and EW(Hα). Fig. 4 shows the relation of the EWs of [OII], [OIII], and [SII] with EW(Hα+[NII]). The EWs of all these lines correlate well with EW(Hα) or EW(Hα+[NII]). The EWs of the Balmer emission lines are considered good tracers of the star formation rate in galaxies (Kennicutt 1983), and it has been shown that [OII] is a good substitute of the Balmer lines in high-redshift galaxies (Gallagher et al. 1989; K92a). Our results indicate that, for practical purposes, any of the EWs displayed in Fig. 4 (except maybe [OIII], which is available for a smaller range of galaxy types) can be used to estimate the star formation rate in normal galaxies, after empirical calibration on the Balmer line EWs. It is worth noting, however, that deriving a star formation rate from an emission line equivalent width is model dependent because, among other things, such a procedure assumes that the ionization is provided by the radiation field from massive stars, which is not necessarily true, specially in early type galaxies (see below). On the other side, the EW of any of these lines is an empirical indicator of galaxy spectral types, given the good correlation between these two quantities, shown in Fig. 3.

It is interesting to compare our Figs. 2 and 4 with Figs. 4 to 6 of K92a, which include all galaxies with emission lines in K92b. Most of the scatter observed in the K92a plots is produced by galaxies not belonging to the sample of normal galaxies discussed here.

3.2. Emission line intensity ratios

Fig. 5 consists of 9 panels showing the behavior of several emission line ratios as a function of the galaxy spectral type. Line ratios are corrected for reddening, as explained in Sect. 2.3.

Fig. 5 shows that very clear trends exist between emission line ratios and spectral types, with very small scatter. Briefly, the trends can be described as follows.

1. Hα/Hβ (panel 5-a) decreases steadily with increasing spectral type. Converted into total extinction at Hβ, this means that C(Hβ) decreases from about 0.7 at ST $\sim$-5 to 0.2 at ST $\sim$ +10.
2. [OII]/Hβ (panel 5-b) first decreases with spectral type, for ST $\lesssim$ -2, then increases slowly.
3. [OIII] is measurable only from ST $\sim$ 1 upwards, where [OIII]/Hβ (panel 5-c) increases very strongly with ST. For ST $\lesssim$ 1 only upper values are available for the [OIII] emission but [OIII]/Hβ seems to decrease in the interval -5 $\lesssim$ ST $\lesssim$ 0.
4. [NII]/Hα (panel 5-d) decreases abruptly for ST $<$ 0, decreasing mildly towards larger values of ST.
5. [SII]/Hα (panel 5-e) also decreases for ST $<$ 0, then increases smoothly for larger values of ST.
6. ([OII]+[OIII])/Hβ (panel 5-f) first decreases until ST $\sim$ 0 (this effect is due to [OII] only since [OIII] is weak in this range of ST), then increases steadily, but with a smaller slope than [OIII]/Hβ. Note that, contrarily to what one might think, the values of ([OII]+[OIII]) for early-type galaxies are not upper values, since in this case the [OII] emission is much larger than the [OIII] emission.
7. [OIII]/[OII] (panel 5-g) increases steadily for ST $\gtrsim$ 1 (the effect of [OIII] is dominant). For lower values of ST only upper values of [OIII]/[OII] are known, but there is a hint that this ratio decreases with ST.
8. [NII]/[OII] (panel 5-h) is roughly constant or decreases slowly until ST $\sim$ 5, decreasing faster for larger values of ST.

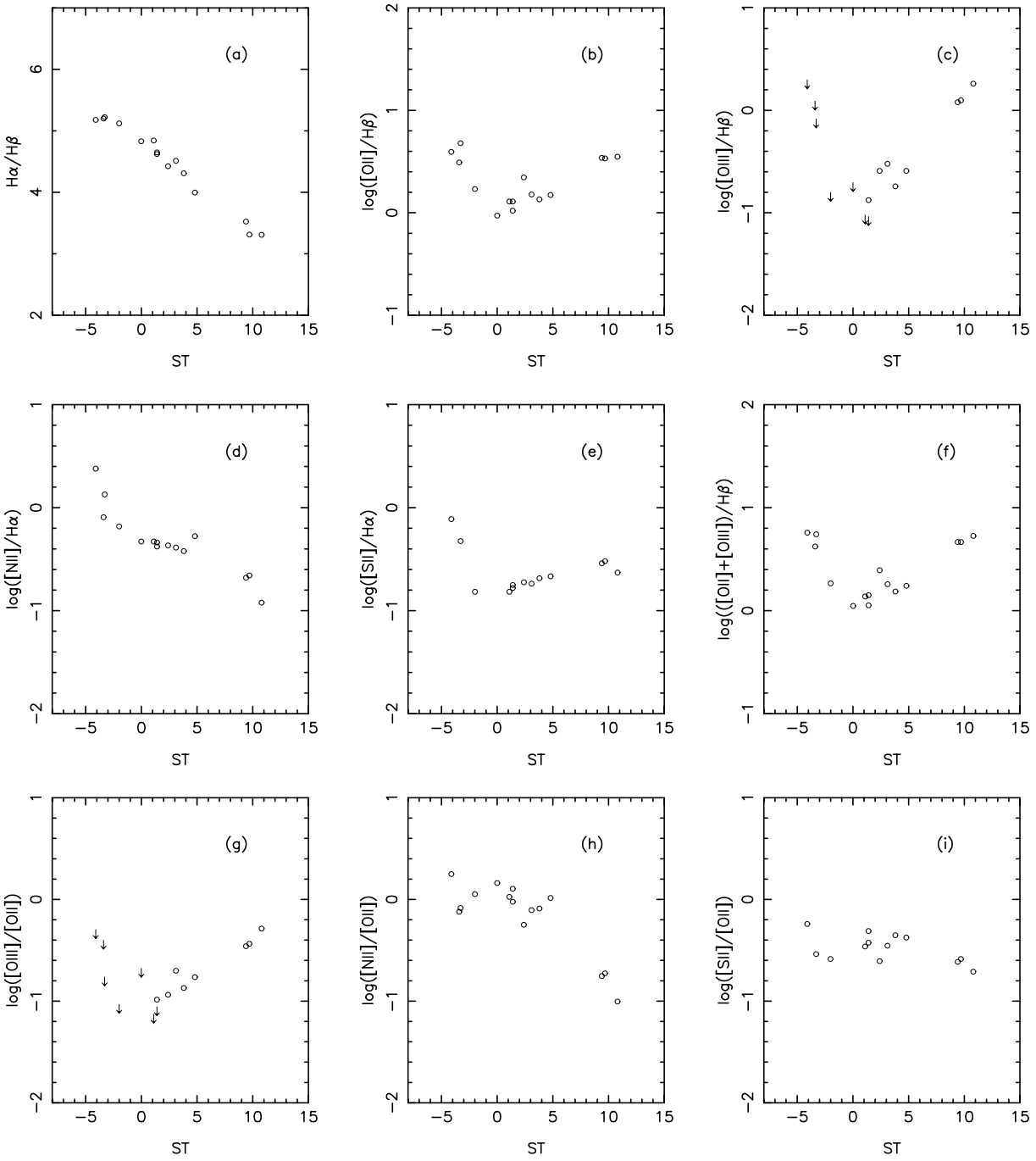

Fig. 5a–i. Behavior of emission line ratios measured in the galaxy integrated spectra as a function of the galaxy spectral type (ST). The line ratios (except Hα/Hβ) are corrected for reddening as described in the text. The emission line ratios in the figure are: **a** Hα/Hβ, **b** [OII]/Hβ, **c** [OIII]/Hβ, **d** [NII]/Hα, **e** [SII]/Hα, **f** ([OII]+[OIII])/Hβ, **g** [OIII]/[OII], **h** [NII]/[OII], **i** [SII]/[OII]. Arrows indicate upper values.

9. [SII]/[OII] (panel 5-i) shows little trend with respect to ST, except, maybe, a slight decrease with increasing spectral types.

The trends seen in Figs. 3 and 5 are impressive, considering that the galaxies were selected simply using a criterion of "normality", and that the ordering by spectral type relies only on the continuum and absorption features of the integrated spectra. However, if we recall that these features reflect the galactic stellar populations, and if the stellar populations obey some simple rules, then it is not so surprising that the emission line properties from integrated spectra can also be ordered. Indeed, emission lines arise due mainly to the presence of hot stars ($T_{eff} \gtrsim$ 30000 K) in the stellar populations, and are modulated by other parameters such as chemical abundances and gas content, which also seem to be related to the general galaxy properties (Roberts & Haynes 1994). Individual HII regions in a galaxy show a def-

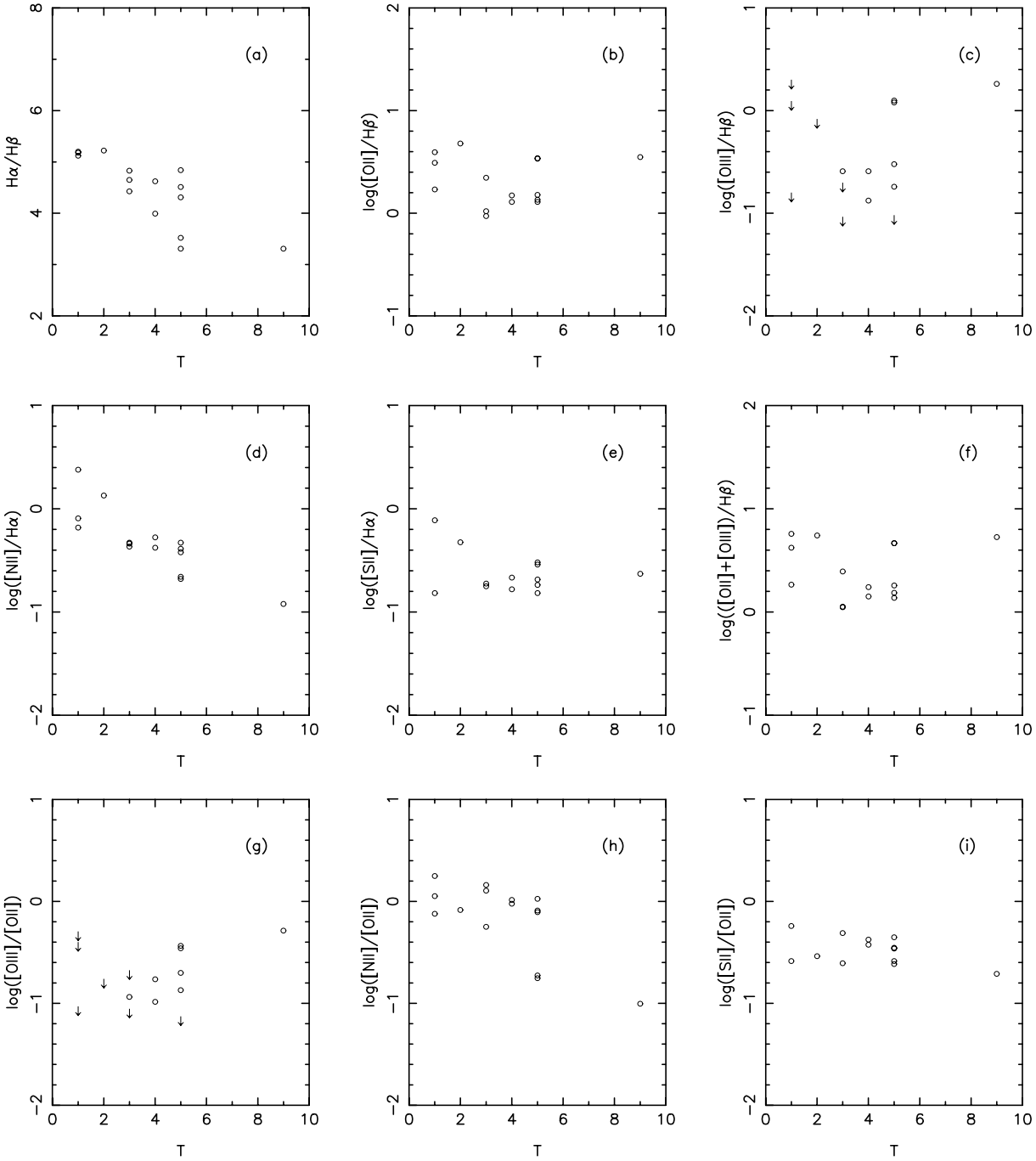

Fig. 6a–i. Same as Fig. 5, but now the line ratios are plotted as a function of the de Vaucouleurs type of the galaxies.

inite scatter in their properties (e.g., Kennicutt & Garnett 1996, Roy & Walsh 1997), but their total number in a galaxy is very large (typically of the order of one hundred) so that the integrated emission line spectrum of a galaxy is well defined. The fact that we find a close link between the emission lines and the continuum and absorption features that are behind the spectral classification suggests that there is a simple relation between the population of hot, ionizing stars and the population of stars responsible for the optical continuum.

It is interesting to see how the emission line ratios behave as a function of the de Vaucouleurs type of the galaxy, which is so far the most widespread way of ordering galaxies and is based on their morphological type. Fig. 6 shows the same line ratios as Fig. 5, but as a function of the de Vaucouleurs T type. One can distinguish trends similar to those seen in Fig. 5, but they are much less clear. That similar trends can be seen is not surprising, since there is some correlation between the spectral sequence and the Hubble sequence (Sodré & Cuevas 1997, Folkes et al. 1996). That the trends are less clear than those in Fig. 5 can be

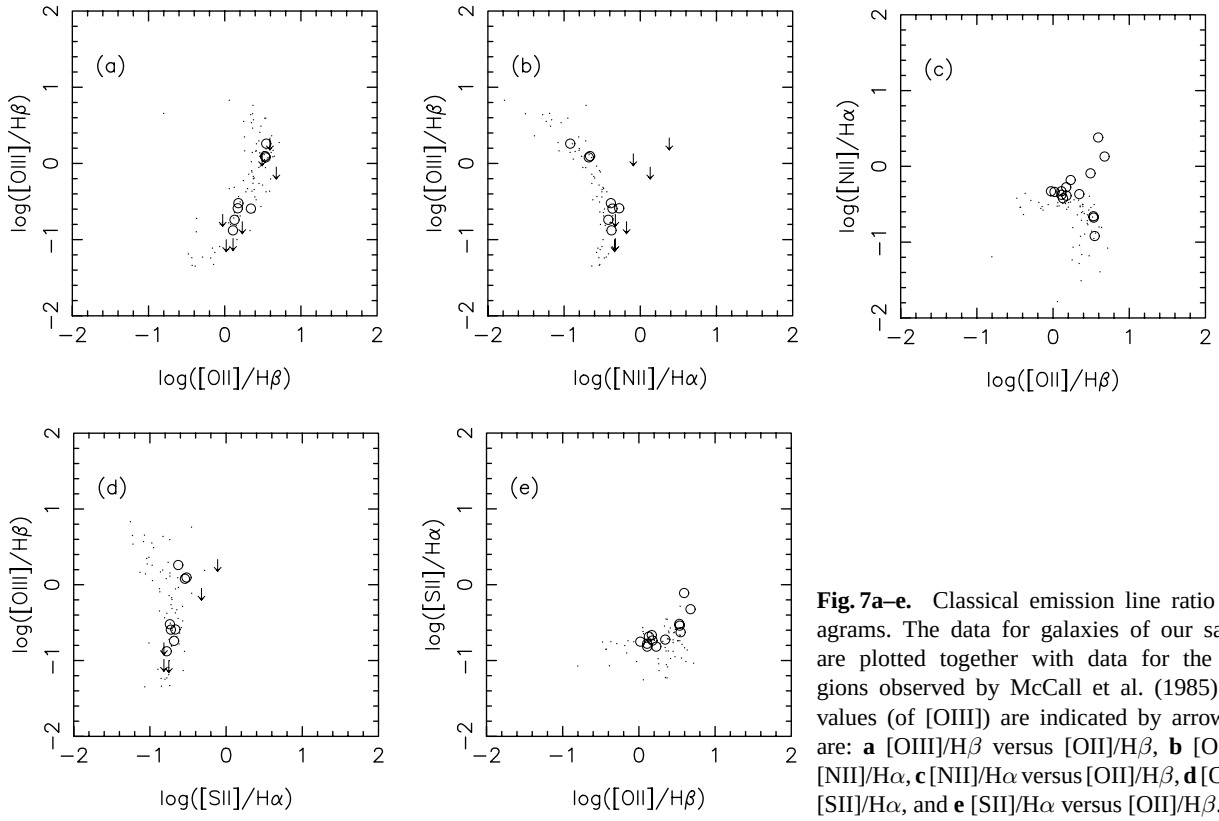

Fig. 7a–e. Classical emission line ratio diagnostic diagrams. The data for galaxies of our sample (circles) are plotted together with data for the giant HII regions observed by McCall et al. (1985) (dots). Upper values (of [OIII]) are indicated by arrows. The panels are: **a** [OIII]/Hβ versus [OII]/Hβ, **b** [OIII]/Hβ versus [NII]/Hα, **c** [NII]/Hα versus [OII]/Hβ, **d** [OIII]/Hβ versus [SII]/Hα, and **e** [SII]/Hα versus [OII]/Hβ.

explained by assuming that the populations of hot stars are not expected to be correlated with galaxy morphological types to the same extent as they are expected to be correlated with the entire stellar populations, as measured by the spectral types.

4. Discussion

Before trying to interpret the trends shown above, it is useful to recall some basics on emission lines and photoionization models. This is done in the next subsection.

4.1. A reminder on emission line theory

Schematically, the (reddening corrected) intensity ratios of emission lines produced in photoionized regions are a function of the following parameters (see e.g. Stasińska 1998 and references therein):

1. the global metallicity, O/H;
2. abundance ratios, like N/O and S/O;
3. the mean effective temperature of the ionizing radiation field $\langle T_{eff}\rangle$;
4. the average ionization parameter $U = Q_H/(4\pi R_s^2 n)$, where Q_H is the number of ionizing photons of an HII region, R_s is the Strömgren radius, and n is the gas density.

The effect of these parameters on the line ratios are the following.

1. Oxygen is the major coolant in HII regions. As O/H increases, the electron temperature decreases because of the increased cooling of the gas. The [OIII]/Hβ ratio first increases (due to an abundance effect), then, for O/H greater than about half solar, decreases due to an electron temperature effect: the gas becomes so cool that the optical [OIII]λ5007 line gets difficult to excite. In this case, cooling occurs through the [OIII] far infrared lines at 52 μm and 88 μm. Qualitatively, the [OII]/Hβ ratio behaves similarly to [OIII]/Hβ, but it is not so reduced at high metallicities, because the cooling is less efficient in the region emitting [OII] than in the region emitting [OIII]. Line ratios like [NII]/Hα or [SII]/Hα are affected by O/H through the electron temperature: they get enhanced as O/H decreases.
2. An increase of N/O only enhances [NII]/[OII], but does not affect the other optical line ratios, since nitrogen contributes little to the cooling at the abundances expected for the general interstellar medium. Similarly, an increase of S/O enhances [SII]/[OII] and leaves the rest unchanged. However, one does not expected S/O to vary among galaxies, since sulfur and oxygen are produced in the same stars. Therefore, any change in [SII]/[OII] should rather be attributed to other causes.
3. The effects of $\langle T_{eff}\rangle$ are twofold. Firstly, $\langle T_{eff}\rangle$ acts on the ionization structure: the proportions of O^+, N^+ or S^+ ions decrease with increasing $\langle T_{eff}\rangle$. Secondly, it influences the thermal balance of the nebula: as $\langle T_{eff}\rangle$ increases, the energy gains become larger and the electron temperature rises, increasing the intensities of the forbidden lines with respect to Hα or Hβ.

4. The effects of decreasing U are to reduce the average ionization, and to decrease ratios like O^{++}/O^{+}. For very low U, such as found in the diffuse interstellar medium, a wide transition zone of low ionization develops, containing O^0 and S^+ ions and still hot enough to allow collisional excitation of optical forbidden lines. Therefore, the [SII]/Hα and the [SII]/[OII] ratios are higher than in HII regions having a large U.

If shocks are present, the emission line ratios are modified. The effect of shocks is to heat the gas to very high temperatures ($T_e = 10^6$–10^7 K). By recombination and free-free processes, this produces a hard radiation field which strongly heats the post shock region, producing an extended, warm, transition region, and enhancing the lines that are most sensitive to the temperature. As a result, [OII]/Hβ, [NII]/Hα, and [SII]/Hα line ratios are enhanced with respect to pure photoionization nebulae.

4.2. Diagnostic diagrams

Line ratio diagrams (Baldwin et al. 1981, Veilleux & Osterbrock 1987) are helpful for the diagnostics of emission line objects. We now use such diagrams to compare the emission properties of galaxy integrated spectra with those of individual giant HII regions. Figs. 7 and 8 show the data from the integrated spectra of the normal spiral galaxies together with those of the giant HII regions (GHRs) observed by McCall et al. (1985) in several spiral galaxies and which compose the GHR sequence. This sequence is interpreted as being a sequence in metallicity (O/H) and also in mean effective temperature or in mean ionization parameter (or both) (McCall et al. 1985, Dopita & Evans 1986). Note that radial abundance gradients, which are a common feature in spiral galaxies (Zaritsky et al. 1994), complicate the interpretation of integrated spectra: the contribution of each annular region is weighted by the luminosities of the HII regions found there and by their spectral properties.

Panel 7-a shows [OIII]/Hβ versus [OII]/Hβ. We see that the points corresponding to the integrated spectra of our standard galaxies that have [OIII] large enough to be observed (i.e. those with ST $>$0) are well inside the GHR sequence.

Panel 7-b displays [OIII]/Hβ versus [NII]/Hα. Galaxies with measured [OIII] emission are disposed along the GHR sequence. The outliers are galaxies for which only upper values of the [OIII] emission are available. They are early type spirals, with ST $<$ 0, as can be deduced from Figs. 5c and 5d. These galaxies stand out conspicuously in the [NII]/Hα versus [OII]/Hβ, diagram (Panel 7c) as well. As will be seen below, we interpret this behavior as being the combined effect of an overabundance of nitrogen in early-type spirals and an ionization source different from ordinary O stars.

Panel 7-d displays [OIII]/Hβ versus [SII]/Hα. In this diagram, while the standard galaxies with measured $\log$([OIII]/Hβ) $<$ 1 are within the HII region sequence, those with $\log$([OIII]/Hβ) $>$1 (i.e. all the galaxies with ST $>$ 9) are slightly to the upper right. This may indicate an increasing contribution of a diffuse ionized medium with increasing galaxy spectral type. Note that Lehnert & Heckman (1994), plotting the spectra of K82a having EW(Hα)$>$ 30 Å in [OIII]/Hβ versus [NII]/Hα and [OIII]/Hβ versus [SII]/Hα planes also concluded that diffuse ionized gas contributes to the integrated spectra of galaxies.[1]

Panel 7-e shows [OII]/Hβ versus [SII]/Hα. The same early-type spirals that show enhanced [NII] emission also show enhanced [SII] emission compared with the GHRs sample of McCall et al. 1985, although to a lesser extent. They are among the ones with the largest [OII]/Hβ ratios. We will argue below that the bulk of the emission in these objects is not due to ordinary O stars.

Fig. 8 shows some line ratios as a function of ([OII] +[OIII])/Hβ. Since the pioneering work of Pagel et al. (1979), the [OII]+[OIII])/Hβ ratio has been widely used to derive the oxygen abundance. In principle, the relation between ([OII]+[OIII])/Hβ and O/H is double sided (e.g. McGaugh 1991, Stasińska 1998). In integrated spectra of galaxies, regions within a few kiloparsecs from the galactic center have probably the greater weight, because most of the star formation is there (Rozas et al. 1996). Since these regions are the most metal rich, one expects that the integrated spectra correspond to the regime where ([OII]+[OIII])/Hβ increases as O/H decreases (but this should be confirmed by simulations).

Panel 8-a shows [OIII]/[OII] versus ([OII]+[OIII])/Hβ. [OIII]/[OII] roughly indicates the ionization state, which is linked to the ionization parameter U, thus to the gas density distribution in each HII region, and to the hardness of the ionizing radiation field. In this diagram, the data points for the integrated galaxy spectra lie well within the region occupied by GHRs except, maybe, for the early spectral type galaxies, with only upper values of [OIII]/Hβ, that tend to locate in the lower envelope of the GHR sequence. The spread of ([OII]+[OIII])/Hβ for the galaxies is smaller than for individual GHRs. This is reasonable, since the integrated spectra are averages over GHRs of various metallicities, ionization parameters and mean affective temperatures.

Panel 8-b displays [NII]/[OII] versus ([OII]+[OIII])/Hβ. We see that all galaxies in the sample fall inside the GHR sequence in Fig. 8b, except three that have higher [NII]/[OII] than GHRs of same ([OII]+[OIII])/Hβ. Note that the three exceptions also have high [NII]/Hα and are all the galaxies of our sample that have ST $<$ -3.

Panel 8-c displays [SII]/[OII] versus ([OII]+[OIII])/Hβ. In this diagram, most of the standard galaxies fall inside the GHR sequence (although, as already noted by McCall et al. 1985, the GHR sequence is not so well defined when using [SII]/[OII]

[1] The detection of a diffuse medium is actually not possible using a [OIII]/Hβ vs [NII]/Hα diagram. Indeed, photoionization models (Stasińska 1998) shows that decreasing the ionization parameter alone to very low values does not shift the points out of the GHR sequence. On the other hand, this diagram is sensitive to the N/O ratio which, unlike S/O, is expected to vary significantly from object to object. Detailed spectroscopic observations of the diffuse intergalactic medium in spiral galaxies (Wang et al. 1997) however suggest that the ionization of this medium cannot be entirely attributed to radiation from O stars.

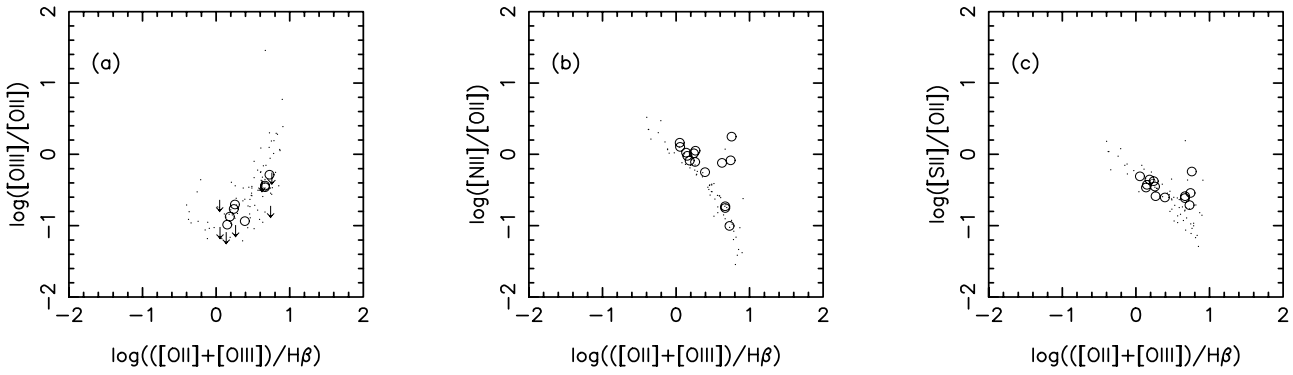

Fig. 8a–c. Forbidden line ratios as a function of the O/H indicator ([OII]+[OIII])/Hβ. The data for galaxies of our sample (circles) are plotted together with data for the giant HII regions observed by McCall et al. (1985) (dots). Upper values (of [OIII]) are indicated by arrows. The panels are: **a** [OIII]/[OII] versus ([OII]+[OIII])/Hβ, **b** [NII]/[OII] versus ([OII]+[OIII])/Hβ, and **c** [SII]/[OII] versus ([OII]+[OIII])/Hβ.

instead of [NII]/[OII]), the galaxies with ST $<$ -3 tending to be above that sequence.

4.3. A tentative interpretation of emission line trends with galaxy spectral types

While the trends between the emission line properties in the integrated spectra of normal spiral galaxies and spectral types are impressive, their interpretation is not necessarily straightforward, since it is dependent on the physical state and spatial distribution of the gas and of the ionization mechanisms.

It was shown by Zaritsky et al. (1994) that the characteristic oxygen abundance in a spiral galaxy derived from its individual giant HII regions increases towards earlier morphological types. The trend seen in Fig. 5f for ST $>$ 0 corresponds (at least qualitatively) to what is expected. Using the Zaritsky et al. (1994) calibration of ([OII]+[OIII])/Hβ into O/H, it would translate into a decrease in the average O/H by $\sim$0.5 dex for ST going from 0 to 10. This is only an indicative value, because the presence of abundance gradients makes it impossible to be more informative without numerical simulations. The case of the galaxies with ST $<$ 0, will be discussed later.

Zaritsky et al. (1994) have also found a strong correlation between the characteristic oxygen abundance and galaxy luminosity (see also Vila-Costas & Edmunds 1992; Roberts & Haynes 1994). Due to the strong correlation between galaxy luminosity and Hubble type in their sample, it is impossible to know which of these two quantities is the primary cause of the correlation. It is interesting to point out that, in the sample of galaxies discussed here, there is no such correlation between O/H and luminosity (most of the galaxies in Table 2 have M_B in the narrow range between -19.9 and -20.7, see K92b) and that the correlation between luminosity and spectral type, if existent, is at most weak. This suggests that O/H is rather linked to the stellar populations, as measured by the spectral types, than to galaxy luminosity.

The increase of [OIII]/[OII] with spectral type (Fig. 5g) for ST $\gtrsim$ 0 is probably due to an increase of $\langle T_{eff} \rangle$ (or an increase of U) when O/H decreases, similarly to what is invoked for individual GHRs (e.g., Garnett & Shields 1987).

The increase of [NII]/[OII] with decreasing spectral type (Fig. 5h) is probably due to an increase of N/O. Indeed, in GHRs, the fact that [NII]/[OII] increases with decreasing ([OII]+[OIII])/Hβ is interpreted, using photoionization models, as being due to an increase of N/O with O/H (Thurston et al. 1996). It is likely then, that in the spectral sequence of galaxies there is an increase of the average N/O with decreasing spectral type, linked with the increase of O/H. This is in qualitative agreement with a secondary production of nitrogen. *A priori*, one cannot exclude the fact that the increase of [NII]/[OII] with decreasing spectral type could be simply attributed to the decrease of O/H (i.e., with N/O staying constant), due to the thermal properties of GHRs. Indeed, [NII]/[OII] = (N/O) (ϵ(NII)/ϵ(OII)), where ϵ(NII) and ϵ(OII) are the emissivities of the [NII] and [OII] lines, and ϵ(NII)/ϵ(OII) is a decreasing function of the electron temperature, thus an increasing function of O/H. Note, however, that the three early-type galaxies that are out of the GHR sequence in Figs. 7c, 7e, and 8b, must have particularly high N/O, because their large [NII]/[OII] cannot be due to a particularly low electron temperature, since [NII]/Hα is large as well.

The ratio [SII]/[OII] does not present any significant trend with spectral type (Fig. 5i). This is consistent with the assumption that the abundance ratio S/O is constant, since both S and O are primary elements. There is a hint of a decrease in that line ratio with increasing spectral type but this may be ascribed to the variations of the ionization parameter along the sequence more than to variations in the relative abundances of S and O.

The increase of [OII]/Hβ as the galaxy spectral type decreases from 0 downwards (as well as that of [SII]/Hα and [NII]/Hα, Figs. 5b, d, e) is very interesting. Early spectral type galaxies appear as upper limits in the [OIII]/Hβ versus [OII]/Hβ diagnostic diagram, since their [OIII] emission is weak. They stand out completely from the giant HII region sequence in diagnostic diagrams with [NII] or [SII]. The integrated spectra of these galaxies are similar to those of LINERs.

Interestingly, 11 of the 15 galaxies of our sample have had their nuclear regions observed by Ho et al. (1997). Their classification of these nuclei into LINERs (L), Seyfert 2 (S2) and HII regions (H) is as follows (see Table 1): all the H type nuclei correspond to ST $>$ 0, while NGC3623 and NGC3368 (ST $<$ -3)

correspond to LINERs. NGC3147 (ST = 0.0) has a S2 nuclear spectrum and NGC3627 (ST = 1.4) has a transition spectrum (T2/S2). The other galaxies in Table 1 have not been observed by Ho et al. (1997). So, the integrated spectra of the galaxies with earliest spectral types have characteristics of LINERs, and the nuclear regions of these galaxies too (we have checked that the contribution of the LINER nuclei to the integrated galaxy spectra is negligible). This seems to indicate that what gives rise to the LINER phenomenon, at least in the normal galaxies we are studying here, is not specifically related to the nucleus.

Given the evidence presented above that metallicity, as measured by O/H, decreases along the spectral sequence, it would be tempting to attribute the distinct behavior of the galaxies having ST < 0 in Figs. 5, 7, and 8 to over-abundances in the gas. But, as stated in Sect. 4.1, over-abundances would produce low [OII]/Hβ, not large ones as observed.

Another possibility is that the distinctive features presented by early type galaxies are due to the aging of the stellar populations associated with GHRs. Sodré & Cuevas (1997), using the spectral synthesis code GISSEL (Bruzual & Charlot 1995), have shown that the spectral sequence of galaxies is well reproduced if one assumes that the star formation rate has the form $\exp(-t/t_*)$, where t_* is an increasing function of the galaxy spectral type. Such a model explains, at least qualitatively, why the equivalent width of Hβ emission increases with increasing galaxy spectral type, as found in Sect. 3. For galaxies with the earliest spectral types, most of the star formation has occurred long ago, and very few O stars are present. In this case, the radiation field in the Lyman continuum may be dominated by post-AGB stars (e.g. Bressan et al. 1994), because, in simple starburst models, these stars provide most of the ionizing photons for bursts older than $\sim 10^8$ yr. This radiation field is much harder than that produced by the massive O stars that power classical HII regions. It is available to ionize the gas bound in the primitive HII regions or the diffuse material produced by their eventual disruption. Binette et al. (1994) have shown that the emission line properties (EWs and line ratios) of early type galaxies can be accounted for by photoionization by such a stellar population. A similar model could well explain at the same time the high [OII]/Hβ, [SII]/Hα, and [NII]/Hα found in the early spectral type galaxies of our sample.

The long lasting dispute about the ionization mechanism in LINERs - photoionization versus shocks - is not settled yet, precisely because under certain conditions both explanations can account for the observed emission line spectra. Models of evolving stellar populations that estimate the energy release in supernovae and stellar winds (e.g., Leitherer & Heckman 1995) will help in the solution of the problem.

We have seen that the effective extinction coefficient at Hβ, $C(\mathrm{H}\beta)$, decreases steadily with increasing spectral type. The beautiful trend shown in Fig. 5a is somewhat surprising, since it is not commonly believed that early-type spirals have higher average extinction than galaxies of later types. Indeed, the related issue of the overall opacity in galaxies has been subject of significant debate, often with contradictory opinions (e.g., Valentjin 1990, Davies & Burstein 1995). Wang & Heckman (1996) have verified that the dust opacity, measured from the ultraviolet to far-infrared luminosity ratio, increases with increasing galaxy infrared luminosity. Taking into account that the far-infrared luminosity is approximately constant for early morphological type spirals and decreases slowly towards later morphological types (e.g., Roberts & Haynes 1994), the correlation noticed by Wang & Heckman might indicate that the dust opacity is indeed decreasing towards later morphological types, in qualitative agreement with the results reported here.

Now, assuming for simplicity that dust properties are invariant with galaxy spectral type, this trend suggests that the mean surface density of dust in galaxies decreases along the spectral sequence from early to late spectral types by a factor of 4. Since the mean surface density of neutral hydrogen in normal galaxies increases towards later types (Roberts & Haynes 1994), the dust-to-gas ratio must be decreasing as the spectral type increases. This is consistent with the idea of dust being formed less efficiently in low metallicity environements, as shown observationally by Lisenfeld & Ferrara (1998). Note that some of the scatter in Fig. 5a may be produced by the random inclination of the galaxies and that the far infrared properties of normal galaxies actually suggest some variations of the dust properties with galaxy type (Sauvage & Thuan 1994).

5. Summary

We have analyzed the global emission line properties of normal spiral galaxies from their integrated spectra. Initially, we have selected from the Kennicutt's atlas (K92b) 23 galaxies which do not present any sign of spectral or morphological peculiarity. A PCA based only on continuous and absorption features of the integrated spectra of these galaxies enabled us to define the galaxy spectral types. We have then considered the subsample of 15 galaxies whose integrated spectra in K92b revealed emission lines. All these galaxies are spirals. We have studied the progression of the properties of these emission lines with galaxy spectral type.

Our major results are the following:

1. The EWs of all the lines correlate well with EW(Hα). As a consequence, for practical purposes, the EW of any of the studied lines ([OII]λ3727, Hβ, [OIII]λ5007, Hα, [NII]$\lambda\lambda$6548, 6583, and [SII]$\lambda\lambda$6717, 6731) can be used to estimate the average massive star formation rate, at least for galaxies with spectral types $\gtrsim 0$. Galaxies with lower spectral type have emission line spectra resembling low excitation LINERs and, consequently, estimates of their global star formation rate based on the their emission lines are unreliable.
2. The EW of all lines correlate very well with ST, suggesting that they can be used as indicators of galaxy spectral types.
3. Emission line ratios present a remarkable regularity when plotted against galaxy spectral types. This stems from the fact that the strengths of the emission lines are linked to the stellar populations, and the latter constitute the basis of the spectral classification of galaxies. The plots are much noisier when using ordinary morphological types.

4. For galaxies with ST $\gtrsim 0$, the increase of (OII+OIII)/Hβ with increasing spectral type suggests a decreasing average metallicity along the spectral sequence.
5. The increase of [OIII]/[OII] with increasing spectral type may be due either to an increase of the mean effective temperature of the ionizing stars, $\langle T_{eff} \rangle$, or to an increase of the characteristic ionization parameter U.
6. The increase of [NII]/[OII] with decreasing spectral type is probably due to an increase of the average N/O. This behavior is consistent with the fact that, in giant HII regions, N/O increases with O/H.
7. The ratio [SII]/[OII] is essentially constant with spectral type and is consistent with S/O being constant. This is expected because S and O are both primary elements.
8. The integrated spectra of early-type spirals (ST $\lesssim 1$) are similar to those of LINERs. The long characteristic time for star formation in early-type spirals as derived by Sodré & Cuevas (1997) provides a natural explanation in terms of ionization by post-AGB stars. Interestingly, in several of these galaxies, the nuclei themselves have been characterized as dwarf LINERs in the work of Ho et al. (1997).
9. The extinction by dust in HII regions seems to decrease with increasing spectral type. This may be a direct consequence of the decrease in mean metallicity along the spectral sequence.

While the interpretation of the trends found with spectral type is only tentative, the reality of these trends is beyond any doubt.

This work confirms that the spectral classification is useful in the analysis of galaxy properties, being able to replace, with advantages, the traditional morphological classification for many purposes. It produces an objective, quantitative and easy to implement classification, that may be more satisfactory for the analysis of large data bases than the subjective and hard to obtain morphological types. Also, since spectra are closely linked to the physics of the stars and of the interstellar medium that build up galaxies, spectral types are more adequate than morphological types for a quantitative approach in studies of galaxy properties, as shown by this work.

Acknowledgements. LSJ benefitted from the support provided by FAPESP, CNPq and PRONEX/FINEP to his work, and warmly acknowledges the hospitality and support of Observatoire de Meudon, where most of this work was realized.

References

Baldwin J.A., Phillips M.M., Terlevich R.J., 1981, PASP 93, 5
Barbaro G., Poggianti B.M., 1997, A&A 324, 490
Belley J., Roy J.R., 1992, ApJS 78, 61
Binette L., Magris C.G., Stasińska G., Bruzual A.G., 1994, A&A 292, 13
Bromley B.C., Press W.H., Lin H., Kirshner R.P., 1998, preprint
Bressan A., Chiosi C., Fagotto F., 1994, ApJS 94, 63
Bruzual G., Charlot S., 1995, Galaxy Isochrone Synthesis Spectral Evolution Library (GISSEL95), available from the authors
Connolly A.J., Szalay A.S., Bershady M.A., Kinney A.L., Calzetti D., 1995, AJ 110, 1071
Cuevas H., Sodré L., Capelato H.V., Quintana H., Proust D., 1998, in preparation
Davies J., Burstein D., 1995, The Opacity of Spiral Disks. Dordrecht, Kluwer
de Lapparent V., Galaz G., Arnouts S., 1998, preprint
de Vaucouleurs G., de Vaucouleurs A., Corwin H.G., et al., 1991, Third Reference Catalogue of Bright Galaxies (RC3). Springer-Verlag, Berlin-Heidelberg-New York
Dopita M.A., Evans I.N., 1986, ApJ 307, 431
Folkes S.R., Lahav O., Maddox S.J., 1996, MNRAS 283, 651
Galaz G., de Lapparent V., 1998, A&A 332, 459
Gallagher J.S., Bushouse H., Hunter D.A., 1989, AJ 97, 700
Garnett D.R., Shields G.A., 1987, ApJ 317, 82
Heckman T., Balick B., Crane P., 1980, A&A 40, 295
Ho L.C., Filippenko A.V., Sargent W.L.W., 1997, ApJS 112, 391
Hubble E., 1936, The Realm of Nebulae. Yale Univ. Press, New Haven
Isobe T., Feigelson E.D., Akritas M.G., Babu G.J., 1990, ApJ 364, 104
Keel W.C., 1983, ApJS 52, 229
Kennicutt R.C., 1983, ApJ 272, 54
Kennicutt R.C. 1992a, ApJ 388, 310
Kennicutt R.C. 1992b, ApJS 79, 255
Kennicutt R.C., Tamblyn P., Congdon C.W., 1994, ApJ 435, 22
Kennicutt R.C., Garnett D.R., 1996, ApJ 456, 504
Leitherer C., Heckman T.M., 1995, ApJS 96, 9
Lehnert M.D., Heckman T.M., 1994, ApJ 426, L27
Lisenfeld U., Ferrara A., 1998, ApJ 496, 145
McCall M.L., Rybski P.M., Shields G.A., 1985, ApJS 57, 1
McGaugh S.S., 1991, ApJ 380, 140
Oey M.S., Kennicutt R.C., 1993, ApJ 411, 137
Pagel B.E.J., Edmunds M.G., Blackwell D.A., Chun M.S., Smith G., MNRAS 189, 95
Roberts M.S., Haynes M.P., 1994, ARA&A 32, 115
Rozas M., Knapen J.H., Beckman J.E., 1996, A&A 312, 275
Roy J.R., Walsh J.R., 1997, MNRAS 288, 715
Sandage A., 1961, The Hubble Atlas of Galaxies. Carnegie Institute of Washington, Washington, DC
Sauvage M., Thuan T.X., 1994, ApJ 429, 153
Sodré L., Cuevas H. 1994, Vistas in Astron. 38, 287
Sodré L., Cuevas H. 1997, MNRAS 287, 137
Stasińska G., 1998, In: Cayatte, Thuan (eds.) Dwarf Galaxies and Cosmology. Editions Frontieres, in press
Thurston T.R., Edmunds M.G., Henry R.B.C., 1996, MNRAS 283, 990
Valentijn E.A., 1990, Nat 346, 153
Veilleux S., Osterbrock D., 1987, ApJS 63, 285
Vila-Costas M.B., Edmunds M.G., 1992, MNRAS 259, 121
Wang B., Heckman T.M., 1996, ApJ 457, 645
Wang J., Heckman T.M., Lehnert M.D., 1997, ApJ 491, 114
Zaritsky D., Kennicutt R.C., Huchra J.P., 1994, ApJ 420, 87
Zaritsky D., Zabludoff A.I., Willick J.A., 1995, AJ 110, 1602